Chapter Two – Data Driven Spots – Algorithm and Implementation

Introduction

The Data-Driven Spots (DDS) visualization technique displays sets of single-valued functions, $F_k(x,y)$, overlaid in a single multi-layer image. Each function is sampled spatially by a 2D array of Gaussians (Gaussian sampling array) before display, which reduces visual obstruction of one variable by another. The sampled function may be displayed either as a semi-transparent colored layer over a gray surface (DDS alpha-blending) or as bumps that protrude from the surface (DDS bump-mapping). When the variable is displayed with transparency, high data values increase the opacity of the layer, i.e. the saturation when combined with the gray background. When the variable is displayed with a bump-map, high data values increase the apparent height of the bumps. Examples of three different data sets are shown on the next pages.

Figure 2.1 presents an example with the habitat ranges of the Mexican free-tailed bat and the Eastern red bat. The data is binary (having only two values) with values of 1 where the bats are found to live and 0 otherwise, as shown in the upper left. The two bats share habitat only along the South-east and Gulf coasts, as far west as Texas. The data is publicly available from the National Atlas of the United States [2003].

Figure 2.2 presents an example of a scanning electron microscope (SEM) image of a geological sample that was processed to reveal the composite elements; in the example two elements, iron and sulfur, are shown. The iron layer has 32 distinct values, the sulfur layer has 87 distinct values; both range in value from 0 to 1.0, much of the variation in the data is due to the substantial amount of noise present in the data. The SEM data was given to our research group by colleagues at EDAX, Inc [2003].

Scanning electron microscopes (SEM) and atomic force microscopes (AFM) scan a sample in a raster pattern and acquire data values at each grid point location – thus the data does not need resampling to fit the *i,j* grid points. A typical grid resolution for an SEM is 500x500 data values; for an AFM, 300x300 data values.

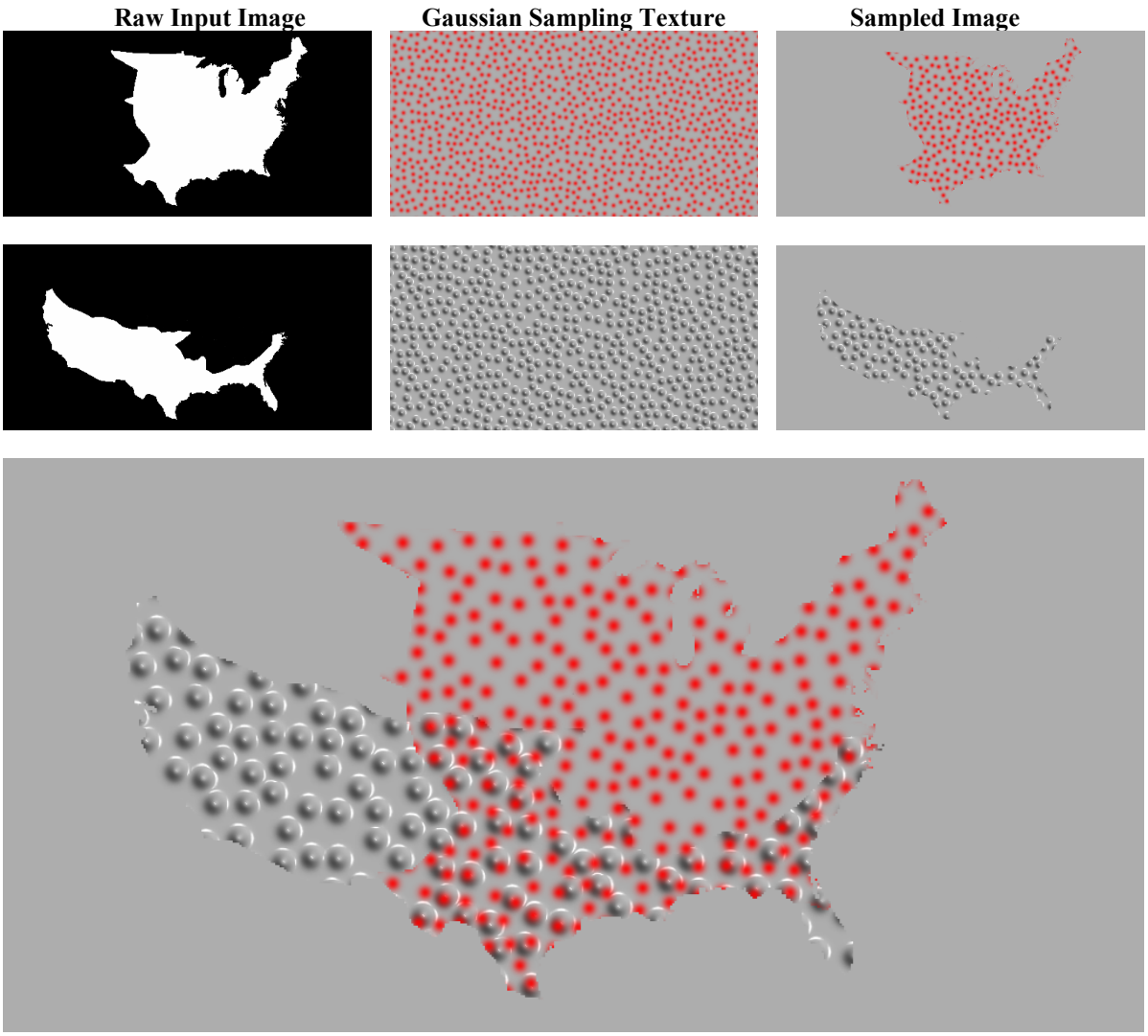

Figure 2.1: The images in the top row show DDS alpha-blending for the habitat range of the Eastern red bat, the images in the middle row show DDS bump-mapping for the habitat rage of the Mexican free-tailed bat. The bottom image shows the two DDS layers combined. The data is from the National Atlas of the United States [2003].

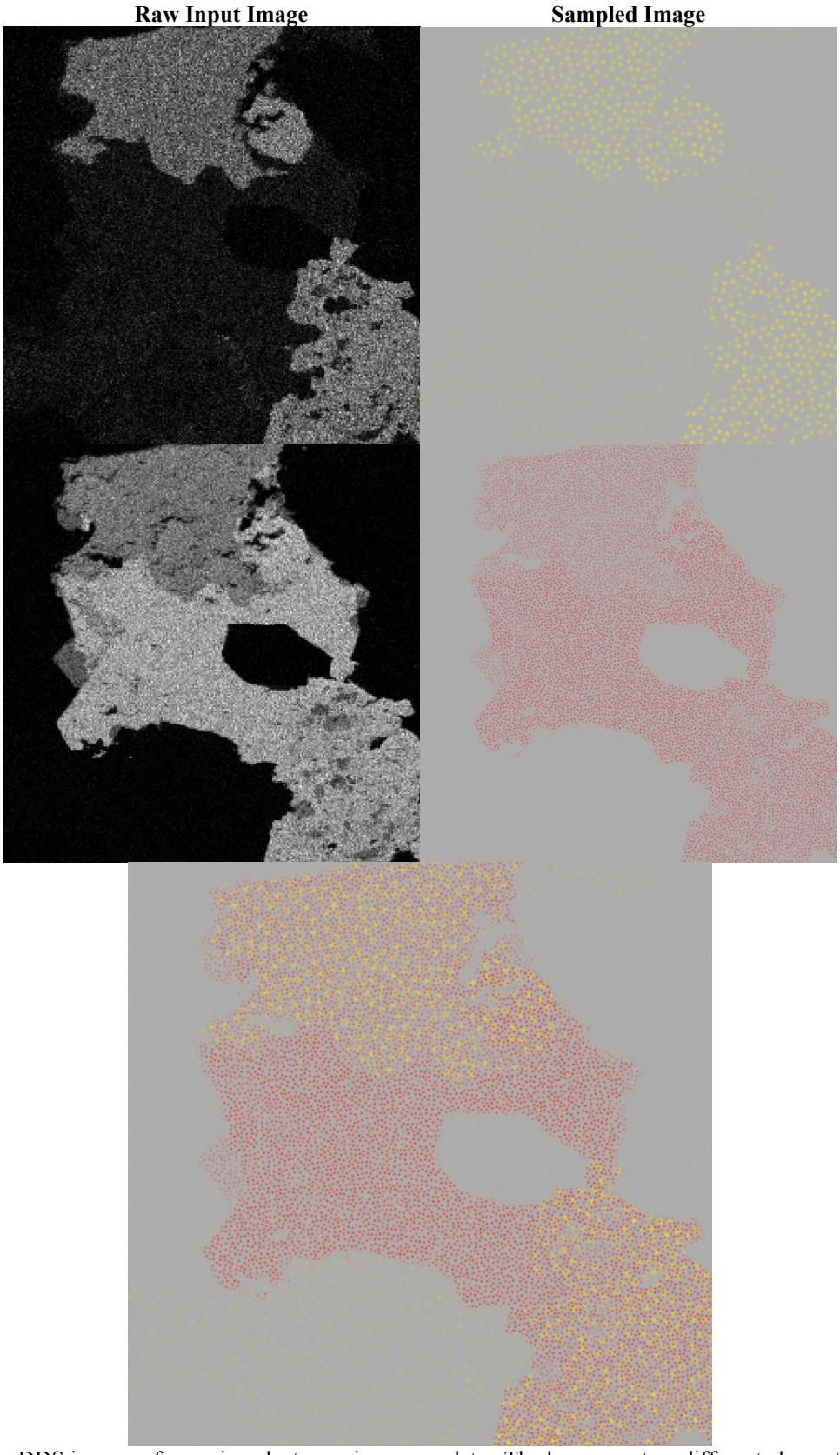

Figure 2.2: DDS images of scanning electron microscope data. The layers are two different elements, iron, shown in the top row, and sulfur, shown in the middle row. Both are displayed with DDS alpha-blending.

Figure 2.3 illustrates data of numbers of beef and dairy cattle per square mile for each of the 48 continental states. There are 44 distinct values of beef cattle and 33 distinct values of dairy cattle for the 48 continental states. The data in Figure 2.3 is from the 1990 census; it is publicly available at the U.S. Census Bureau [2003].

US population data is an example of data that is not acquired at regular grid points – simply because houses are not regularly spaced across the country. US census tracts are clustered around cities and widely spaced in rural areas. How census data should be resampled to fit a regular grid depends on what resolution or what level of detail the person viewing the information wants to see. One common method is to average the data within counties, an example of a *chloroplethic* map. However there is a cost to averaging the data in that the rural-urban boundary may be blurred.

Before data is displayed with either DDS alpha-blending or DDS bump-mapping the data values are normalized to fall in the range of 0 to 1 for alpha-blending or, if the data has negative value, -1 to 1 for bump-mapping. Whether different functions, $F_k(x,y)$, within a given set are normalized independently, based on the individual ranges for each $F_k(x,y)$, or normalized as a set, based on the overall range of values across all k functions, depends on both the nature of the data and the goal of the visualization. Take the SEM data as an example; because the amount of sulfur and iron are elements of a composite whole, if amounts of sulfur and iron are normalized independently, then it is not possible to compare the relative amounts of sulfur and iron. It is necessary to have unit compatibility before two functions are normalized together. For example, temperature and pressure are not measured in the same units and therefore cannot be normalized together. Variables that represent parts of a whole, such as the numbers of different ethnic populations in a city, must be normalized together. Variables that are not parts of a whole, such as the numbers of dairy cattle and the numbers of beef cattle, can be normalized separately or jointly.

The number of levels in a single data set that can be perceived and understood by the viewer is influenced by a variety of factors – the display technique used to display the data, the viewing conditions, various properties of the data itself, and, ultimately, by the person viewing the image. Although a data image may contain many different levels (87 is the most levels in the examples above), the number of levels a person can accurately distinguish, and therefore the number of different data values that person can potentially process, may be quite less.

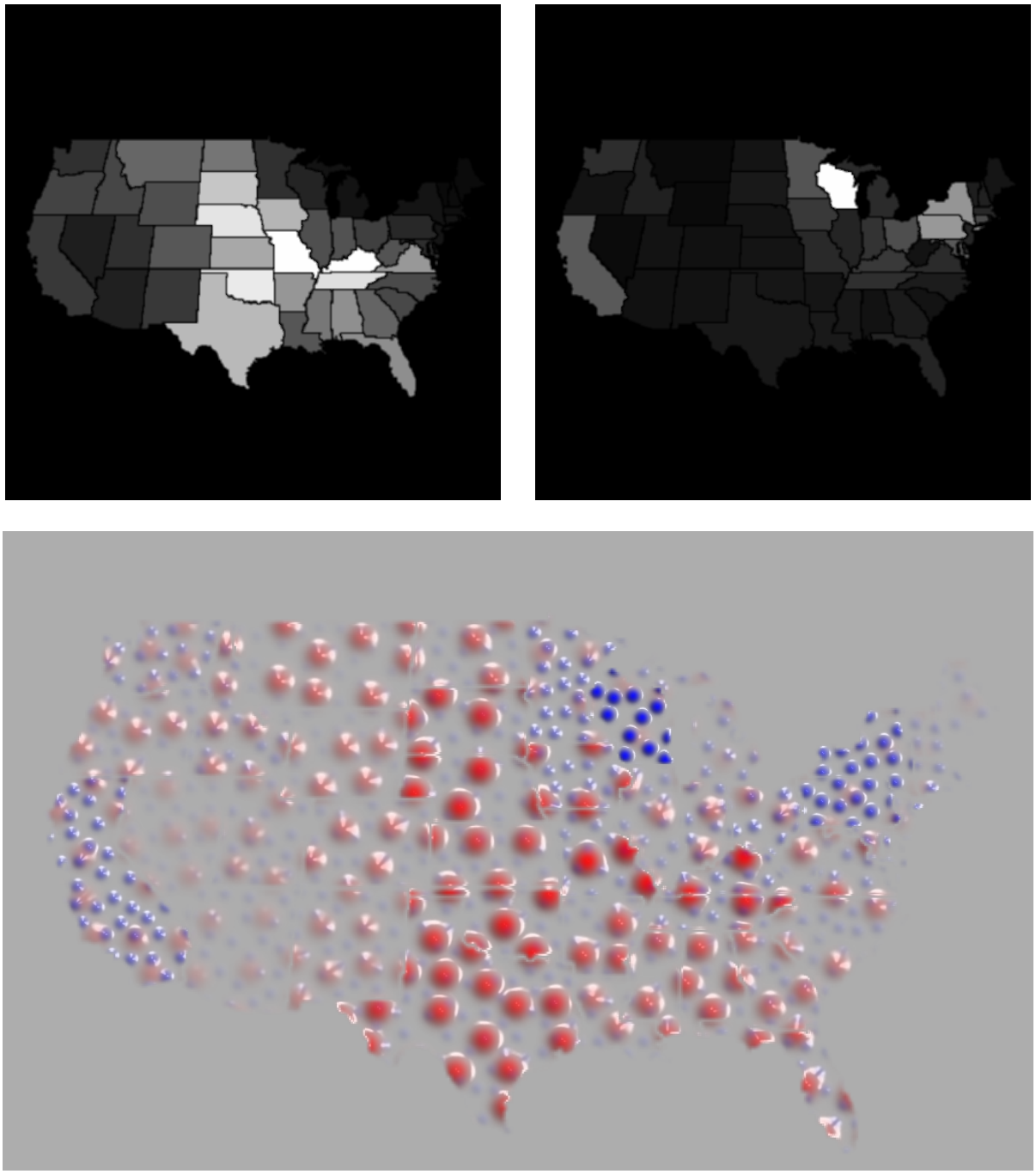

Figure 2.3: The top row is beef cattle and dairy cattle per square mile, from the 1990 census. The bottom image shows the two layers combined: red bumps for beef cattle and smaller, blue, bumps for the dairy cattle. The data is from the 1990 census; it is publicly available at the U.S. Census Bureau [2003].

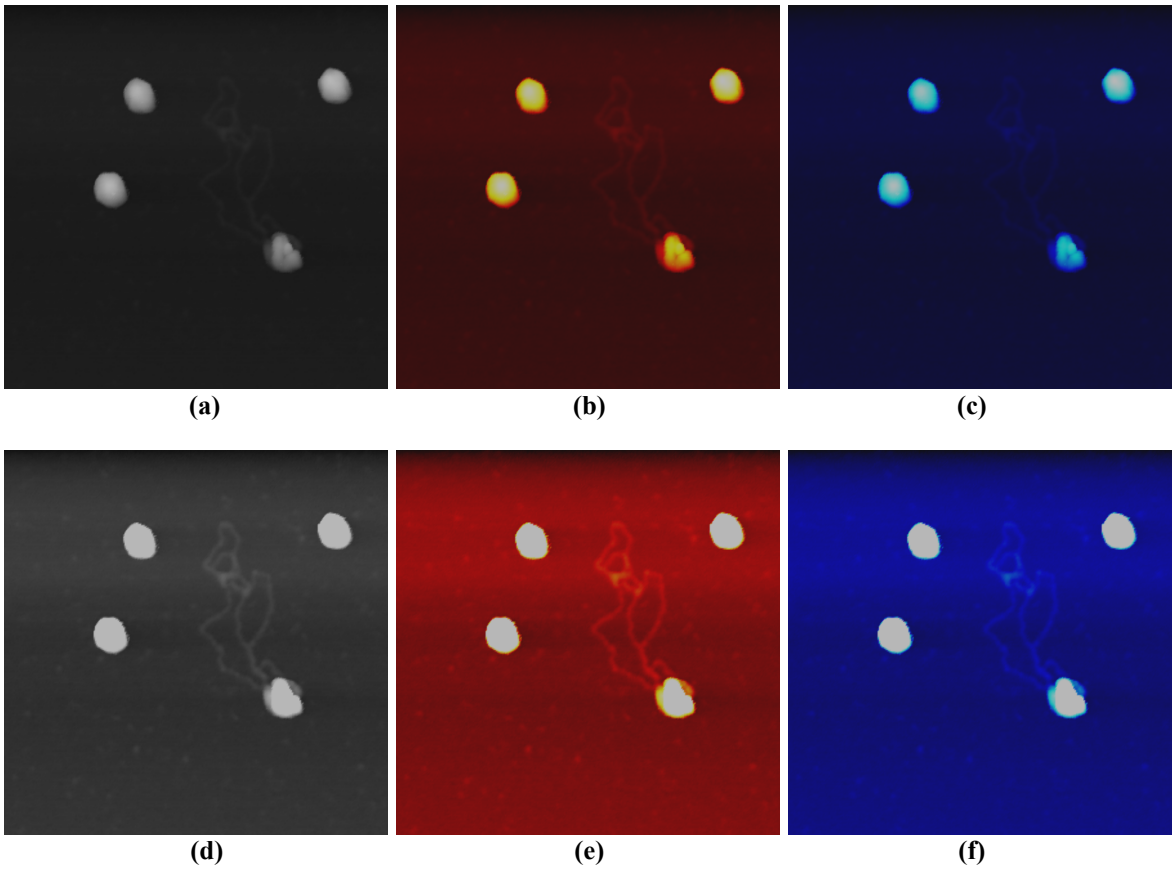

Figure 2.4: Grayscale, red-blackbody, and blue-blackbody color renderings of a AFM images of adenoviruses and DNA. Images a-c show height mapped directly to color, using the full height range, which is approximately 0-100nm. In the bottom row, images d-f, only the height range from approximately 0-30nm is mapped to the color whereas higher values are clamped at the maximum color. The DNA is much easier to see in the bottom row of images.

Grayscale color maps are commonly used to display data; they are easy to implement, and intuitive for the viewer. Grayscale color maps are considered the most direct mapping of scalar data to display, with the minimal loss of information. However, Pizer and Zimmerman [1983] and Pizer [1985] have shown that the perceived dynamic range for images displayed using a perceptually linearized grayscale color map is only about 90 (measured in the number of jnds, or just noticeable difference levels). They compare this result to the perceived dynamic range for the blackbody color map, which they found to be 120. Figure 2.4 shows grayscale, red-blackbody, and blue-blackbody color displays of an AFM image of adenoviruses and DNA.

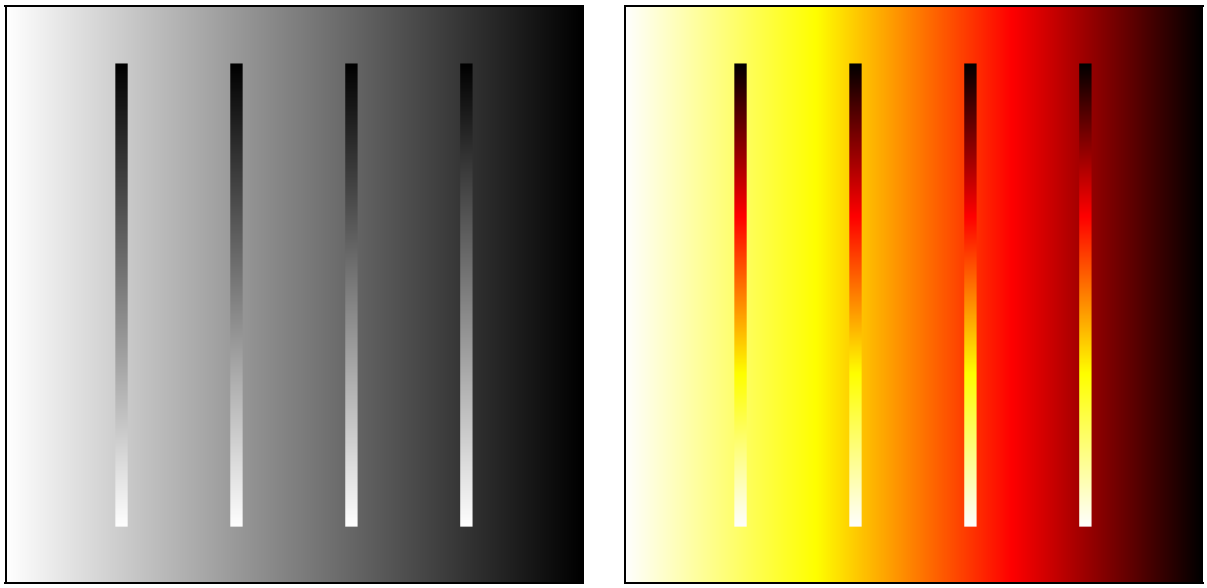

(a) **(b)**

Figure 2.5: The intensity contrast gradient (a) based on [Ware, 2000] shows one problem with using gray values to display data. Each of the vertical intensity gradients is identical, but they look dramatically different due to color contrast effects caused by the background gradient. When gray values are used to display data, two data points of equal value displayed with the same grayscale value may not be perceived as equal if they are surrounded by different gray values. The blackbody color map as in (b) also shows color-contrast effects. Understanding human visual perception is key to creating successful data visualizations.

Whatever color map is used to display the data, Pizer et al. argue that equal changes in the recorded intensity must be perceived as equal changes in the displayed intensity, not just for some ranges of the color map, but across the entire mapping. In other words the color mapping must be perceptually linear [Pizer and Zimmerman, 1983].

Perceptually linearizing color maps turns out to be a tall order, and the downfall of using grayscale or other color maps, such as the blackbody color map, is the perceptual phenomenon of color contrast: "*The most obvious relevance of contrast effects to visualization is that they can result in errors of judgment during the reading of quantitative (value) information that is encoded using a gray scale*" [Ware, 2000, page 80]. Figure 2.5 shows an example of color contrast for both a grayscale color map (based on [Ware, 2000]) and a blackbody color map. In the figure all four vertical gradients are numerically identical – the visual shift in the gradients is caused by the background gradient and is a purely perceptual phenomena. It is difficult to believe that this is true – only by covering the background can one convince oneself.

Contrast effects can also be seen in gradients defined with saturation, which DDS uses to display value information. When gradients defined by saturation but distinguished by different hues are displayed simultaneously, contrast effects are not seen. Figure 2.6 shows four examples: image (a) uses the same color for both foreground and background gradients; (b) uses different colors; (c) contrasts the two target colors used *Color-Color* session of the pilot study and (d) contrasts the two target colors used in the *Color-Color* session of the main study. One might speculate that the greater the angular distance in hue (defined in the HLS color space) the less the gradients suffer from contrast effects. The colors in 2.6 (c) have a smaller angular distance in hue than the colors in (d) and the effect is stronger.

Sampling the data spatially with the Gaussian spots and then applying multiple layers in an image, so that spots are on top of other spots that differ in hue, might actually reduce color contrast effects; DDS may present a new way of looking at data that minimizes error caused by color contrast.

The goal of any visualization technique is to maximize the information the viewer can see and understand accurately. To achieve this goal, human visual perception must be taken into consideration; this is an important theme that runs throughout this dissertation.

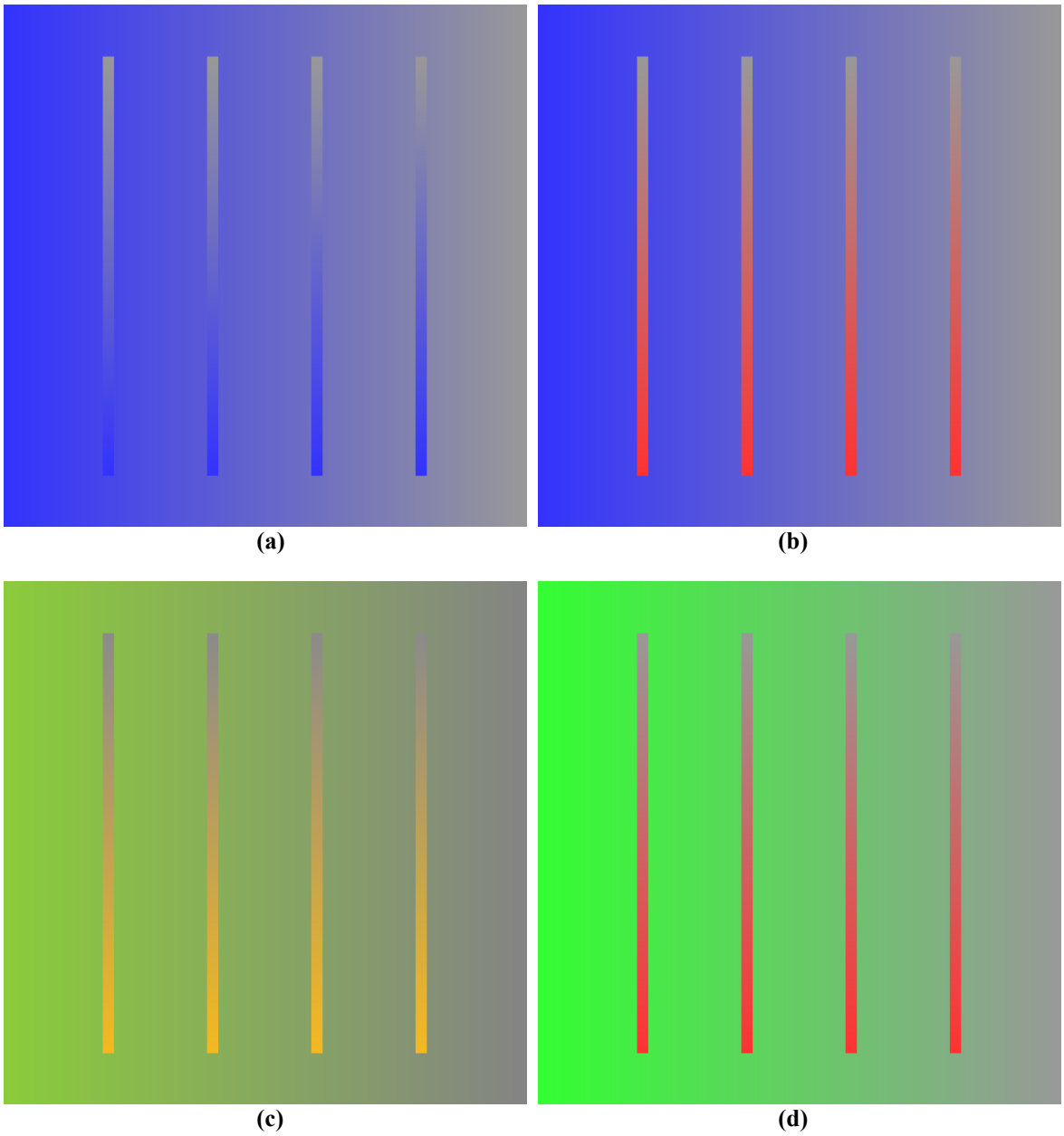

Figure 2.6: Contrast effects in saturation. When the hue is the same for the foreground and background gradients, as in (a), the foreground gradients do not appear the same due to strong contrast effects. When the hue is different for the foreground and background gradients, as in (b), the contrast effect is reduced. The two target colors used in the *Color-Color* session of the pilot study are shown in (c) and the two target colors used in the *Color-Color* session of the main study are shown in (d). Lower contrast effects could be a side-effect of DDS sampling, as Gaussian spots only overlap other Gaussians with different hues.

$$P(x_1, x_2) = \frac{1}{2 \times \pi \times \sigma_1 \sigma_2} \times e^{\left[-\frac{1}{2} \left[\left(\frac{x_1 - \mu_1}{\sigma_1} \right)^2 + \left(\frac{x_2 - \mu_2}{\sigma_2} \right)^2 \right] \right]} \quad 2.1$$

Gaussian Sampling Arrays

Gaussian Function

A single circularly-symmetric 2D Gaussian is generated from a binormal density function with two equal standard deviations $\sigma_1=\sigma_2$ (equation 2.1, Figure 2.7). The Gaussian spot is centered in the image at $x=\mu_1$, $y=\mu_2$. Before they are used to sample the underlying data, different Gaussians are normalized so Gaussians with different standard deviations all have the same maximum value of 1.0 at the center. The normalized Gaussian value is 0.61 at one standard deviation; it is 0.14 at two standard deviations; and 0.01 at three standard deviations.

Placement of the Gaussians in the Sampling Array

All Gaussians in any particular sampling array have the same standard deviation. One Gaussian is generated per array and is placed repeatedly in the array, where each center location is a randomly chosen integral *i,j* point. The details of generating a Gaussian sampling array are described below.

First, the number of Gaussians, *N*, is determined. *N* is a function of both the size of the Gaussian sampling array (image dimensions *width* and *height* in pixels) and the standard deviation of the Gaussian (equation 2.2). The constant *C* controls the maximum density of the Gaussians, for the examples presented in this dissertation it was set to 32.

$$N = width*height / (C * \sigma^2) \quad 2.2$$

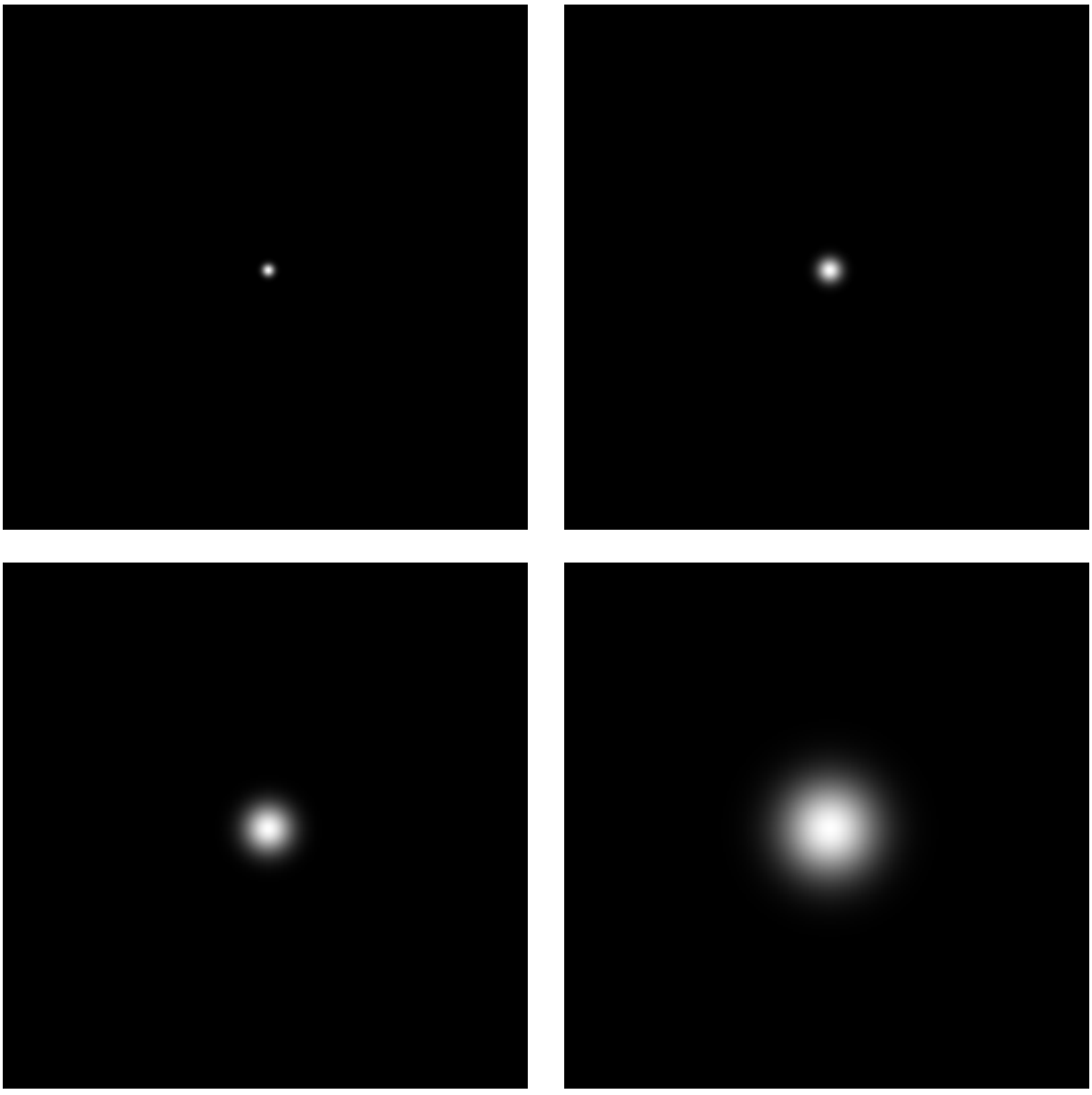

Figure 2.7: Single Gaussians with standard deviation equal to two, four, eight, and sixteen pixels.

The placement algorithm sequentially creates potential *(i,j)* coordinates at which to add a new Gaussian to the array, using a pseudo-random number generator with uniform distribution. The coordinates are checked against each of the existing Gaussians currently in the array. If the new coordinates place the Gaussian at least 4.5 standard deviations from each of the others, it is added. Otherwise, it is discarded and new coordinates are created. This process repeats until all *N* Gaussians have been added to the array.

As 4.5 standard deviations is chosen to be the minimum distance between the center points of two Gaussians, closest Gaussians will intersect at 2.25 standard deviations, where each Gaussian value is 0.08. At this intersection between spots, the maximum level of opacity is 0.16. Most spots are placed greater than 4.5 standard deviations apart, producing regions of greater transparency (less opacity) between spots.

For the examples presented in this dissertation all layers had the same minimum spacing of 4.5 standard deviations and the same constant *C=32*. Choosing these numbers was an empirical process. If the number of spots in an image depends only on the standard deviation and a minimal distance, then the spots are tightly packed in the image – creating a less random-looking spot distribution. Instead, by setting the number of spots less than the maximum that could fit in the image, and by setting the minimum spacing less than that required by a uniform density, the placement algorithm has the freedom to pack spots tightly in some regions of the image and sparsely in other regions of the image, producing a more random-looking spot distribution. Figure 2.8 shows four examples of Gaussian sampling arrays with different standard deviations.

In the development of DDS, I observed that the randomness of the spot spacing was important. A reaction-diffusion technique [Turk, 1991; Witkin and Kass, 1991], which places spots in a naturalistic way, turned out to be not random-looking enough because circular, ring-like patterns of spots appeared. These spurious patterns could be distracting to the viewer. The technique described here is an improvement in that no repeatable patterns in the spots appear. Figure 2.9 compares the spot patterns generated with the reaction-diffusion technique and the random technique described here.

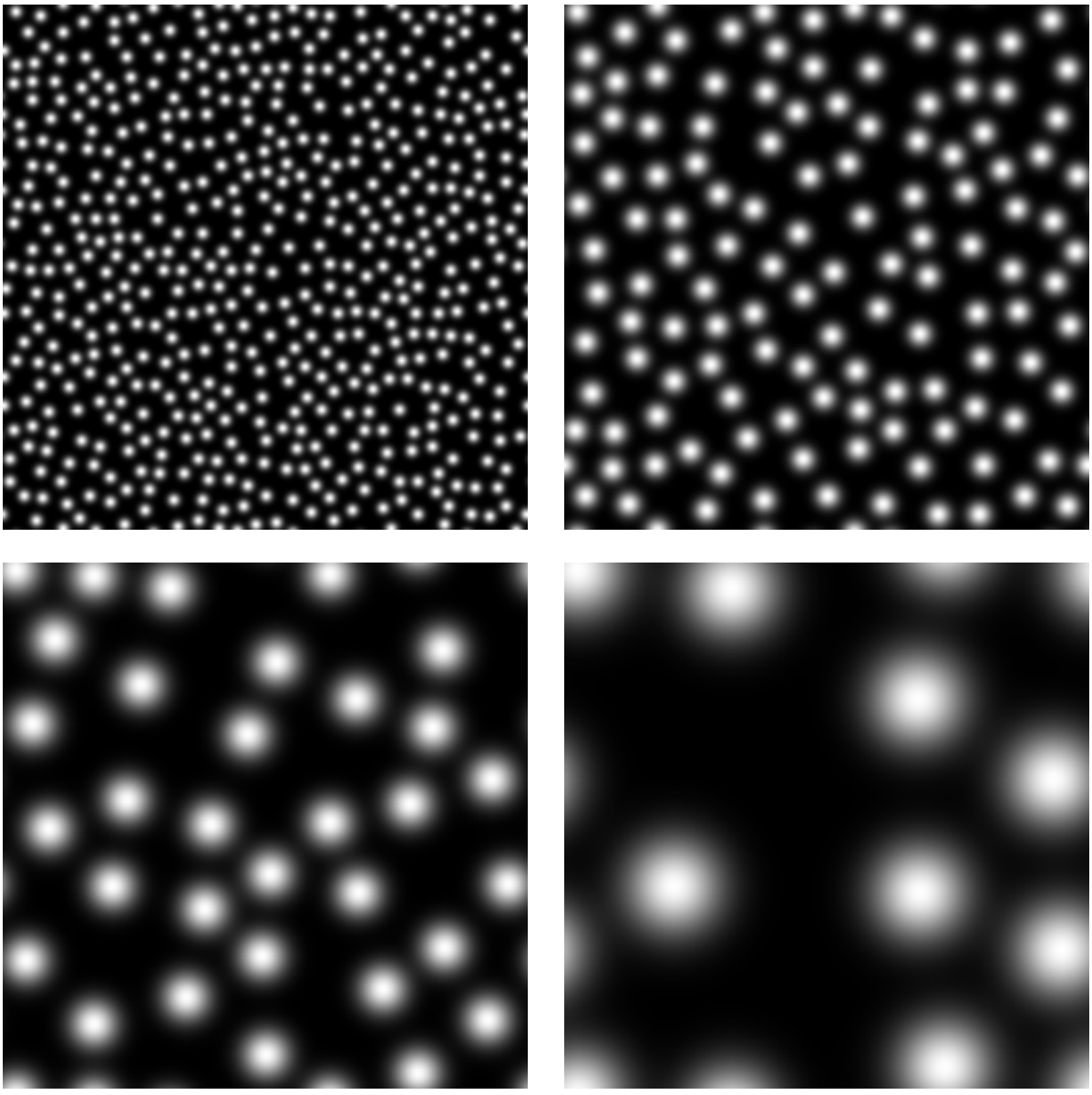

Figure 2.8: Gaussian sampling arrays with standard deviation equal to two, four, eight, and sixteen pixels. The placement algorithm is meant to distribute the spots in a random fashion, so that some areas of the textures are denser and some are sparser.

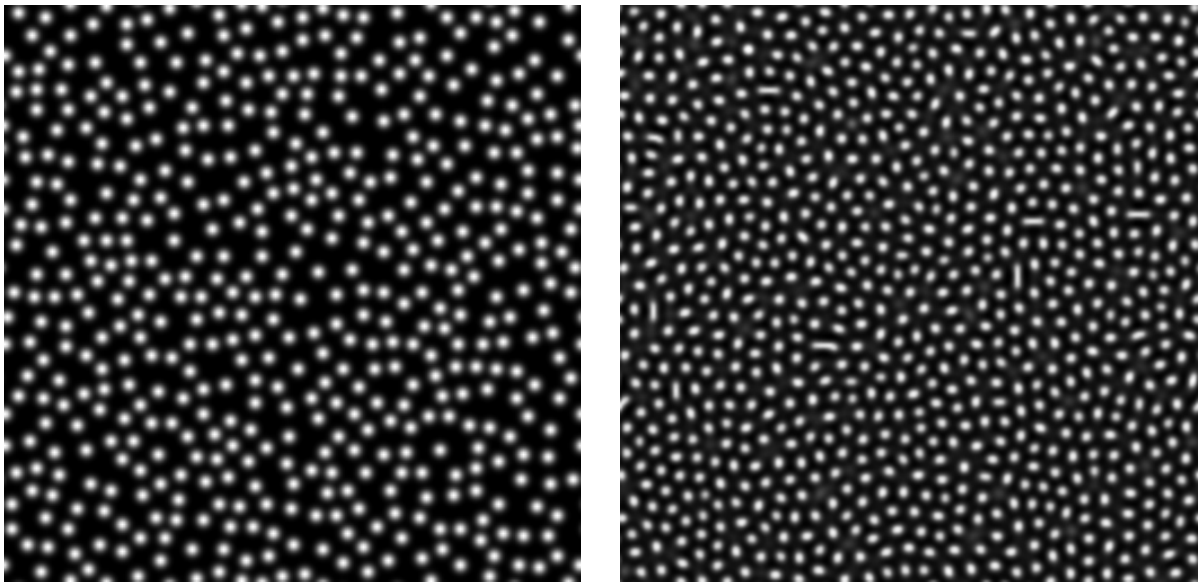

(a) **(b)**

Figure 2.9: Comparison of Gaussian sampling array (a) with the reaction-diffusion textures (b). The two images are comparable in the size of the spots.

The reaction-diffusion technique grows patterns of spots in a process that simulates how spot patterns such as that of a leopard's coat occur in nature. In the texture generation process, each spot influences the spots that surround it. Spot spacing is regular and produces spurious patterns in the data. In addition, the spots do not all have a uniform shape or intensity, as the Gaussian spots do, instead, oblong spots can form and some spots are brighter than others (Figure 2.9b). The Gaussian spot arrays allow for more control over spot shape, intensity, and inter-spot distances and pixel gray scale values, as well as for a more random-looking spot distribution.

The Gaussian sampling technique was implemented after the experimental evaluation of DDS, which uses trial images with reaction-diffusion spots. The experiment shows that the reaction-diffusion spot layers displayed with alpha-blending are visually separable in multi-layer DDS images and that participants are able to accurately perceive shapes sampled with reaction-diffusion spot layers. However, the benefits of more uniform spot shape and intensity, less regular spot placement, and direct control over spot density make the Gaussian sampling technique more appropriate for DDS. In Chapter Three, two trial images are compared, one with reaction-diffusion spot sampling and one with Gaussian spot sampling.

Standard deviation, σ, in pixels	2	4	8	16	32	64
Number of spots	8192	2048	512	128	32	8
Average pixel distance between Gaussians centers	9.67	19.37	38.9	77.9	158	312
Density (% pixels above 2 standard deviations)	0.76	0.76	0.76	0.76	0.76	0.77
Average pixel intensity	0.196	0.196	0.196	0.196	0.196	0.196

Table 2.1: Descriptive statistics of the Gaussian sampling arrays for a variety of Gaussian standard deviations. Gaussian sample array image size was 1024x1024 pixels.

Once the coordinates for all Gaussians are known, the single Gaussian image is added to the array at each coordinate location. The Gaussian sampling array is processed so that the image forms a torus, i.e. the edges of the array wrap around and connect – the top edge wraps to the bottom edge and the left to the right. This attribute of the Gaussian array means that it can be used in standard computer graphics texture mapping and stretched and shrunk without causing artifacts. Because the Gaussian sampling array is on a torus, Gaussians that fall on the edge wrap around to the opposite side.

Generating the Gaussian sampling array as a function of the standard deviation – which determines the number of Gaussians for a given array size as well as the minimum distance between Gaussians – has several benefits. The density of the texture, as measured by the number of pixels with grayscale value above a certain threshold, is independent of the standard deviation. The average value of the Gaussian texture is also independent of the standard deviation. Table 2.1 lists densities as well as the average pixel intensities as a function of standard deviation σ.

A smaller standard deviation yields smaller, more numerous, Gaussian spots, while a larger standard deviation yields larger, less numerous, Gaussian spots. Because the data is sampled by each pixel within the Gaussian spots, a smaller standard deviation leads to a more uniform sample distribution, and a larger standard deviation leads to more clustered sampling.

Visual Perception and Gaussian Sampling Arrays

It is interesting to compare the Gaussian sampling array images to texture images studied in the perceptual psychology literature. Much work had been done in the study of human texture perception, and that work can guide how textures should and should not be used in data visualization and can predict the suitability of the Gaussian sampling arrays for data visualization.

Julesz et al. have written extensively about texture characteristics [Julesz, Gilbert, and Shepp, 1973; Julesz, Gilbert and Victor, 1978; Julesz, 1981; Julesz and Krose, 1988]. Julesz et al. [1973] define a set of statistics to describe the visual properties of texture images. The first three statistics are: 1. the average darkness of a texture area; 2. the probability that both ends of a dipole land on black points; and 3. the probability that all three points of a triangle land on black points. An important property of this statistical definition of texture is that two textures that have the same higher order statistic (i.e. two textures with the same third-order statistic) are guaranteed to have the same lower-order statistics. The converse is also true: if two textures differ in the second order statistic they will differ in the third-order statistic. The authors found that people could not visually discriminate textures that were identical in the first- and second-order statistics but different third-order statistics. In order for textures to be visually distinct, they must differ in at least the second or first-order statistics.

The Gaussian sampling arrays all have the same first-order statistic – they all have the same average image intensity. The probability that both ends of a dipole will land on a black value depends on the spatial distribution of the white and black pixels – this will be different for the Gaussian sampling arrays with small spots than for the Gaussian sampling arrays with large spots (see Figure 1 in Julesz [1973]), thus the Gaussian sampling arrays differ in the second-order statistic and are therefore visually distinct based on the evidence of Julesz et al. [1973].

Julesz [1981], after discovering textures that were easily distinguished despite the fact that they had identical first and second order statistics, revises his theory on texture discrimination based on the statistical properties of textures. His further investigations led him to the conclusion that texture discrimination is based solely on first-order statistical differences of locally conspicuous features – features he calls textons. Textons are defined as elongated blobs of a given width, with three important properties: color, shape (orientation and length), and the presence of terminators (end-points of the elongated blobs). Textures that can be described in terms of different texton properties will be visually distinct – for example, textures that differ in color will be visually distinct, as will two textures that do and do not have terminators. The Gaussian sampling arrays do not have terminators, however two Gaussian sampling arrays will differ in either color or size.

The Brodatz album [1966] is a series of over a hundred photographs of both manmade and naturally occurring textures. While the work of Julesz focuses on mathematically defined textures, Brodatz and others try to determine what visual characteristics of everyday textures are important. Figure 2.10 presents photographs I took that are similar in nature to the ones found in the album. The Brodatz album includes man-made textures of woven fabrics and naturally occurring textures such as pebbles on a beach, the bark of a tree, or piles of leaves.

Several researchers have used the images in the Brodatz album to further investigate the visual dimensions of texture, specifically the characteristics people use to classify the images. Tamura, Mori, and Yamawaki [1978] presented pairs of images from the Brodatz album to people and asked them to rate the two images along six different scales. They found that the dimension along coarse to fine was a strong distinguishing factor. Rao and Lohse [1992, 1993] applied multidimensional scaling techniques to analyze how people clustered images from the Brodatz album. The authors identified three orthogonal dimensions important for texture perception: repetition, orientation, and complexity or granularity. Liu and Picard [1994], also using images from the Brodatz album, develop a mathematical analysis of the textures. They found their method of mathematical decomposition identified the same three perceptual dimensions in the textures that Rao and Lohse found people use: periodicity (regular versus random), orientation, and scale (feature size).

Figure 2.10: Photographs based on images from the Brodatz album [1966]. The top row has textures found in nature, and the bottom row has textures that are man-made.

Spot noise [van Wijk, 1991] is a texture-generation technique that can be used to create textures with the properties found in the Brodatz album. Natural-looking textures are generated by convolving a uniform pattern, such as an "S" or "+" shape with a field of white noise. Figure 2.11 show some examples. The resulting image contains the repetition of the uniform shape, but with the appearance of slight random variations found in natural textures. The benefit of spot noise techniques is that each dimension – repetition, orientation, complexity – can be controlled by a separate input parameter when generating the textures.

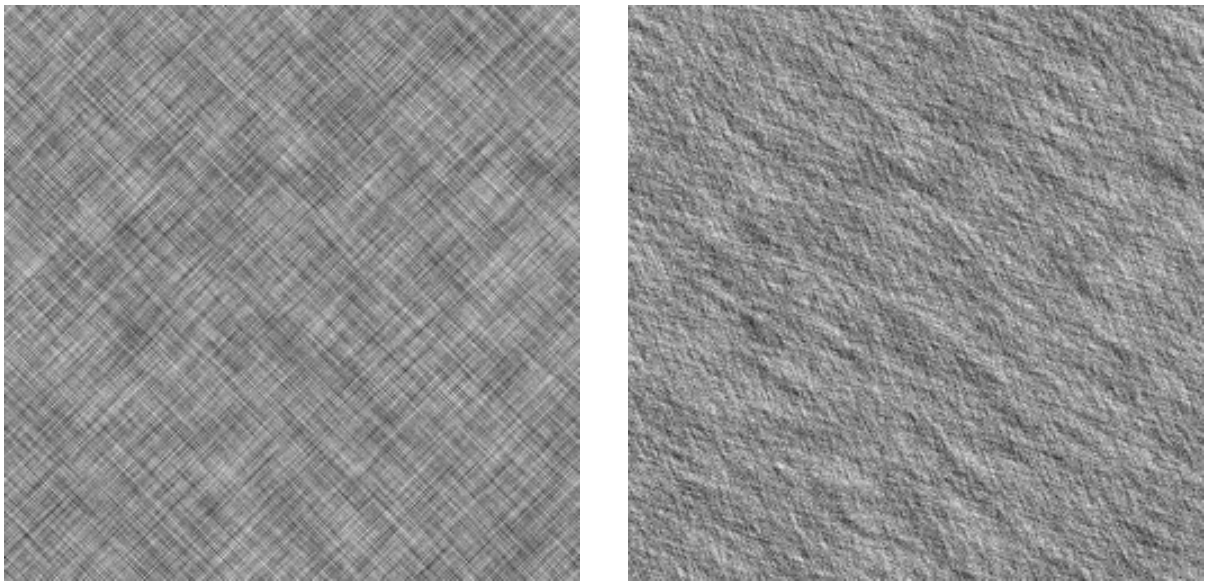

(a) **(b)**

Figure 2.11: Examples of spot noise textures. Texture (a) was created by convolving a '+' rotated 45° with an image of uniform white noise. Texture (b) was created by convolving a rotated 'S' with the same image of uniform white noise. Both textures contain the repetition of the original pattern, but with a natural-looking final result.

Before the development of DDS, our research group looked into using spot noise techniques to generate textures to display data. The idea was that the underlying data values would determine the parameters of the spot noise functions for each (x,y) location in the image. This is similar in spirit to the glyph, or icon, based data visualization techniques, which will be described in more detail in Chapter Four. The basic idea is that the data to be displayed is used as input parameters to a texture-generation technique, either as the parameters of a spot noise texture, or as the parameters for length and orientation of a stick-figure glyph. The final images clearly show patterns in the data – represented by areas in the texture that have different texture dimensions and visual properties. The reason we chose not to pursue this further is that the goal for DDS was that each of the original data variables remain visually distinct in the final image – a property that is true of neither the spot noise nor glyph techniques. However, spot noise is particularly good at illustrating fluid flow [Cabral and Leedom, 1993; de Leeuw and van Liere, 1998].

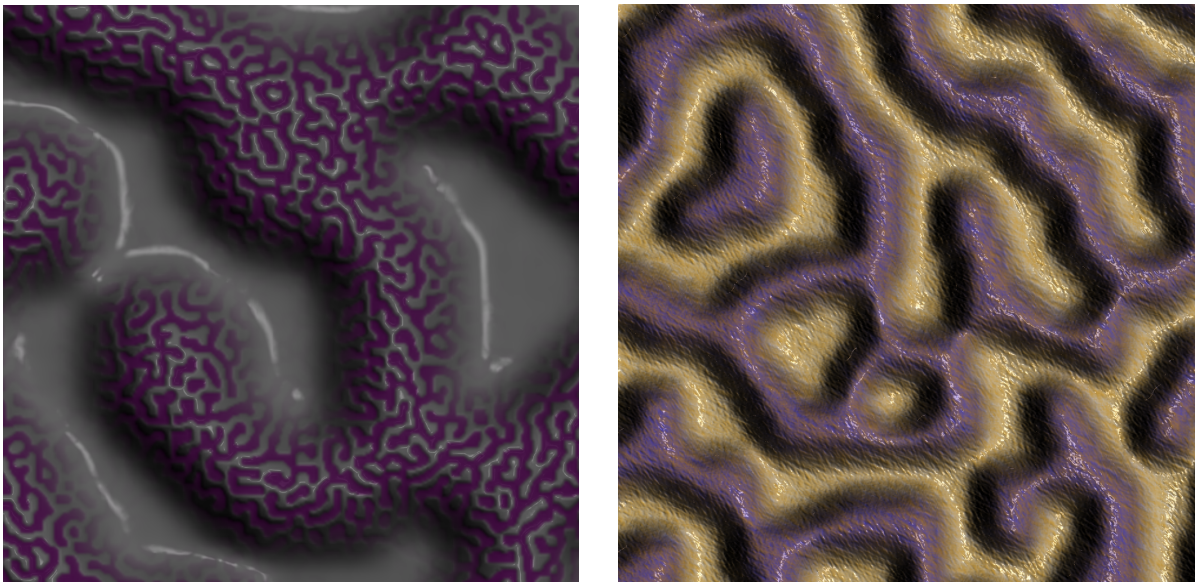

(a) **(b)**

Figure 2.12: Reaction-diffusion stripe patterns. Stripes did not layer as well as spots in our investigations.

The reaction-diffusion textures described in [Turk 1991; Witkin and Kass, 1991] also produce natural-looking textures, Figure 2.12 shows two examples based on stripe patterns. Reaction-diffusion models the cellular differentiation in organic systems through a process of chemical reaction and diffusion. The original model, introduced by Turing [1952], describes the formation of biological patterns based on initial concentrations of chemicals that both diffuse throughout the system and react to one another until stability. Patterns emerge due to the different rates at which the chemicals diffuse. Patterns generated by the reaction-diffusion model have been compared to patterns found in nature such as the stripes and spots on cats, zebras, and giraffes [Witken and Kass, 1991].

While neither Turk [1991] nor Witkin and Kass [1991] address the idea of using reaction-diffusion systems for displaying data, this was one of the first directions we took in our lab for visualizing multiple scalar fields in a single image. Reaction-diffusion models both the initial chemical concentration across a surface and the rates of diffusion or reaction of the chemical layers, which can be different at each point on the modeled surface. Reaction-diffusion can visualize data by using that data to set the values for the chemical concentrations and diffusion rates and producing a spot or stripe image based on those values. It is difficult to say what reaction-diffusion shows in the data, the hope is that underlying patterns emerge that correlate with data values.

Ware and Knight [1992, 1995] termed orientation, size and contrast the *Primary Orderable Dimensions* of visual texture. Ware's work has bridged the fields of perceptual psychology and data visualization. In his work in the field of data visualization he has investigated using display elements based on Gabor functions, which are the product of a sine wave grating and a circularly symmetric Gaussian. The Gabor functions were chosen because they simulate the receptive fields of neurons in the early visual system that are tuned to orientation detection.

Ware and Knight [1995] map up to three spatial variables to the orientation, size, and contrast parameters of the Gabor function, which is used to randomly sample the variables in space, similar to DDS but much more densely packed. The authors claim that these three texture characteristics are the primary dimensions in texture perception, in that variations in orientation, size or contrast, will be more visible than variations in other texture dimensions, such as regularity and symmetry [Ware and Knight, 1995]. This technique is useful for displaying static images of flow fields, and the authors demonstrate it by displaying magnetic field data.

Interestingly, Ware points out that the three texture dimensions, size, contrast, and orientation, although perceptually orthogonal, are also intrinsically linked. For example, when contrast is zero, neither size nor orientation is visible, and when the size of the element is small, orientation is difficult to see [Ware and Goss, 1992].

In earlier investigations, we considered mapping one spatial variable to the height of the Gaussian, as for the DDS bump-mapped layers, while mapping another spatial variable to the width of the Gaussian, which stretched the Gaussians from circular to elliptical. As described in Chapter Four, Ware [2000] describes such a mapping of data to display element as integral, because shape characteristics such as length and width are not processed independently, but form a holistic unit. I found it difficult to see the two variables separately, when they mapped to the height and width of the Gaussians.

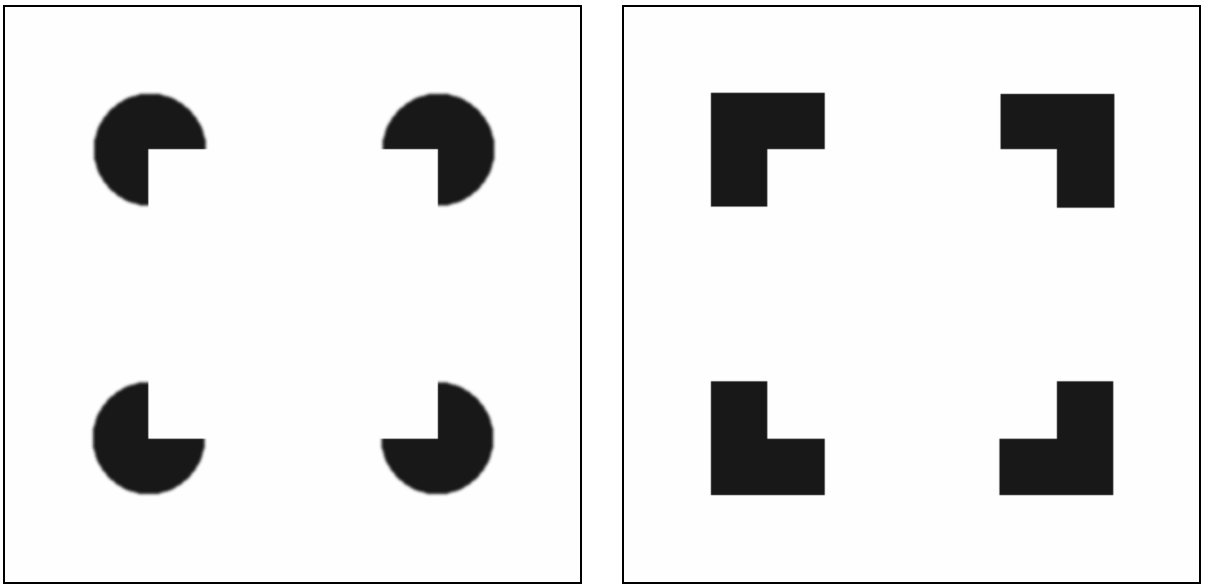

(a) **(b)**

Figure 2.13: "Magic Square" images based on [Hoffman, 1998]. The subjective square is stronger in the images on the left, due to the cusps in the circular inducers. Although (b) also has cusps, they are less unique and are attributed to the underlying inducers instead of the subjective square.

Why Spots?

Through experimentation during the development of the DDS technique, I found that textures such as the examples from the Brodatz album, spot noise, and reaction-diffusion stripes are not suitable as visually separable layers, because the textures are too complex visually. Yet, the question remains: Why spots? Why not use a different underlying display element, such as an ellipse or a square, one that is replicated throughout the texture and does not change in size with the data? Is the spot shape a critical component to the success of the DDS technique?

Figure 2.13 illustrates one of the reasons Gaussian spots are used as the underlying texture feature in the Gaussian sampling arrays instead of another shape primitive, such as a square. Both the spot simplicity of shape and continuity of form mean the spot is an ideal inducer of subjective contours – this is clear in Figure 2.13(a) where the illusory square on the left is much more strongly visible than the one on the right. The cusps in 2.13 (a) appear to be caused by an overlapping square, whereas the cusps in 2.13 (b) appear to be part of the underlying shape. The key difference is that the cusps in 2.13 (a) create a discontinuity in the circle inducers – something that our visual system treats is less likely, whereas the cusps in 2.13 (b) occur in the underlying inducer and therefore our visual system does not need to create the overlapping square to explain the cusps visually. [Hoffman, 1998]

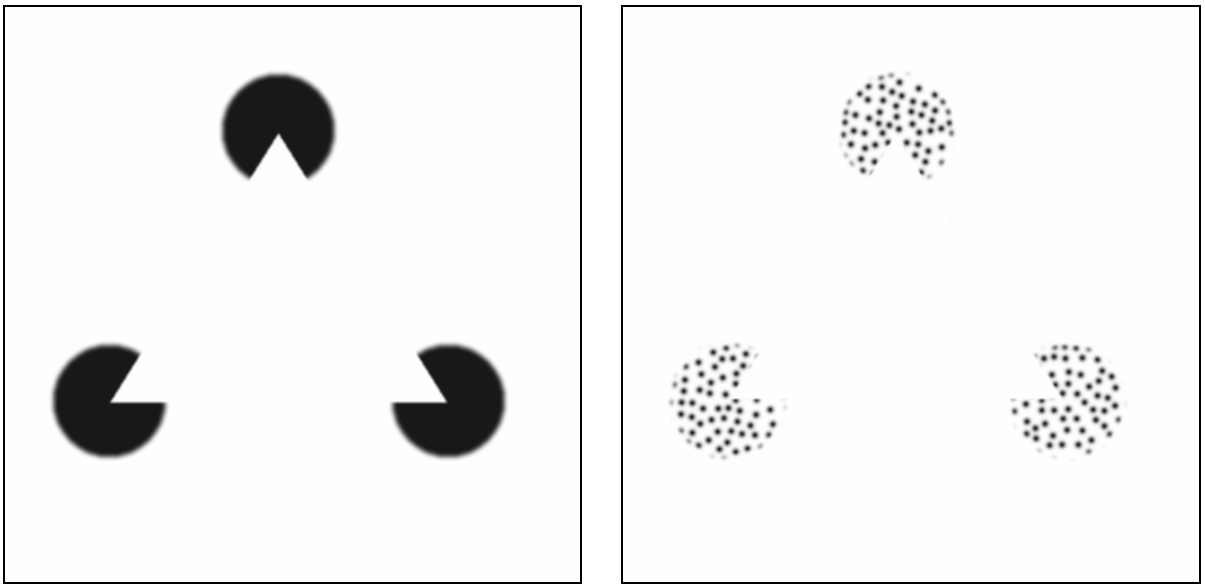

Figure 2.14: The Kinazsa triangle (a) and the Kinazsa triangle induced by collections of spots (b) (image based on [Kennedy and Ware, 1978]).

Kennedy and Ware [1978] showed that illusory contours could be created by collections of spots as the inducers, as in Figure 2.14. When spots are grouped together to make a good figure, as defined by the area of Gestalt psychology, strong subjective contours occur. The images in their paper are the first evidence that a technique like DDS could work. DDS, by using spots as the underlying sample unit, produces strong subjective contours along data boundaries. This is a powerful way to harness human visual perception for data display.

Textures suffer from the same contrast effects found in color images and discussed earlier. Figure 2.15, based on Ware and Knight [1992], shows this effect. To counteract this texture size contrast effect, DDS uses a unique hue for each spot layer, which provides a redundant cue for grouping spots within each layer.

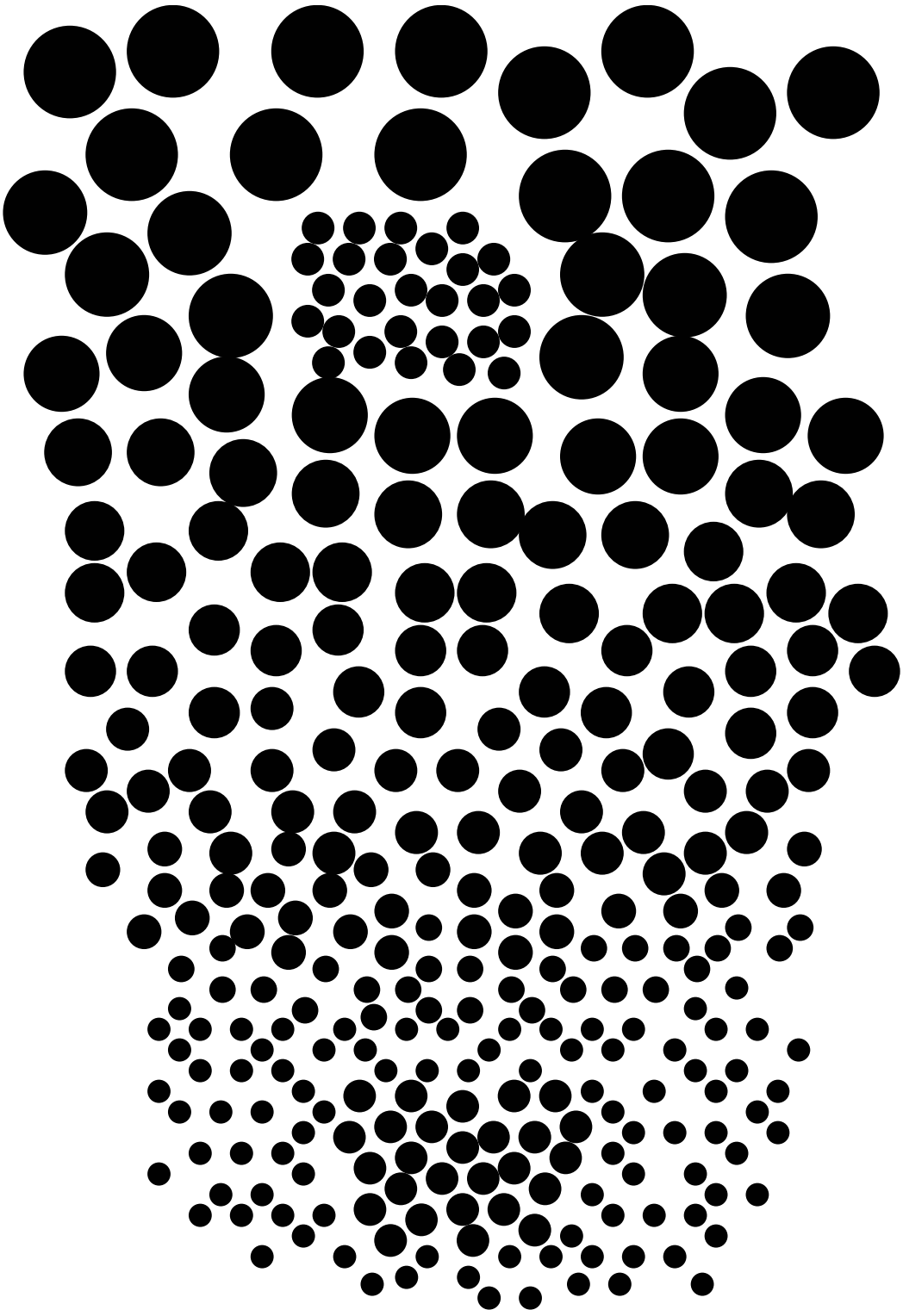

Figure 2.15: Texture size contrast image based on [Ware and Knight, 1992]. Notice the apparent size difference when the medium-sized spots contrast with large versus small spots.